3.12 TURBULENCE DECAY IN THE STABLE ARCTIC BOUNDARY LAYER

Andrey A. Grachev *
University of Colorado CIRES / NOAA Environmental Technology Laboratory, Boulder, Colorado
Christopher W. Fairall
NOAA Environmental Technology Laboratory, Boulder, Colorado
P. Ola G. Persson
University of Colorado CIRES / NOAA Environmental Technology Laboratory, Boulder, Colorado
Edgar L Andreas
U.S. Army Cold Regions Research and Engineering Laboratory, Hanover, New Hampshire
Peter S. Guest
Naval Postgraduate School, Monterey, California
Rachel E. Jordan
U.S. Army Cold Regions Research and Engineering Laboratory, Hanover, New Hampshire

1. INTRODUCTION

Understanding and proper parameterization of sub-grid scale fluxes in the stable boundary layer (SBL) are of obvious importance for climate modeling, weather forecast, environmental impact studies and other important applications. In the very stable boundary layer atmospheric turbulence is suppressed that allows buildup of high concentration of contaminants. In such conditions, the impact of atmospheric pollutants and potential chemical and warfare agents reach a maximum (e.g. Mahrt, 1999).

As stability increases, turbulence decays and vertical fluxes vanish. However behavior of turbulent fluxes and other characteristics including determination of the critical Richardson number are poorly understood in the very stable conditions. This study uses turbulence data collected over the Arctic pack ice during the Surface Heat Budget of the Arctic Ocean Experiment (SHEBA) to examine the turbulence decay in the SBL.

The SHEBA field program, which occurred from October 1997 to October 1998, was the most ambitious scientific effort ever attempted in the Arctic and the SHEBA flux-profile data is the largest single data set ever collected in the atmospheric surface layer. Turbulent fluxes and mean meteorological data were continuously measured at five levels, nominally 2.2, 3.2, 5.1, 8.9, and 18.2 m (or 14 m during most of the winter), using a 20-meter main tower and also at 4 portable automated measurement sites at various locations near the ice camp. These data were supported by a wealth of atmospheric, oceanographic, and ice/snow data. The SHEBA measurement program was highly successful. Eleven months of the measurements during SHEBA cover a wide range of the stability conditions, from the weakly unstable regime to very stable stratification, that allow us to study the physical nature of the SBL in detail including the very stable cases.

Andreas et al. (1999) and Persson et al. (2002) provide detailed description of the SHEBA site, deployed instruments and obtained data.

2. EVOLUTION OF THE SBL

Usually the very stable states observed during SHEBA were associated with light winds and clear skies during both dark and sunlit periods. Figures 1 and 2 show typical one-day time series of the basic meteorological variables and fluxes for the very stable conditions observed during two polar seasons. The data are based on 1 hour averaging. During the dark period (Fig. 1) stable conditions are long lasting and can reach quasi-stationary states compared to the sunlit period (Fig. 2). The Arctic SBL during the sunlit period is associated with the nocturnal cooling. Toward sunset, as the solar elevation and radiation reaching the surface decline, the near surface temperature begins to drop, leading to cooling of the diurnal mixed layer. The time series of the temperature measured at the five levels (Fig. 2c) display how the near surface air becomes stably stratified. This behavior is similar to the temperature evolution in the traditional nocturnal boundary layer observed at mid-latitudes. Figures 1f and 2f show the time series of the bulk Richardson number defined as

$$\mathrm{Ri}_B = -\frac{gz}{T_v}\frac{\Delta\theta + 0.61T_v\Delta q}{u^2}\ , \qquad (1)$$

* *Corresponding author address:* Dr. A. A. Grachev, NOAA/ETL, R/ET6, 325 Broadway, Boulder, CO 80305-3328, e-mail: Andrey.Grachev@noaa.gov

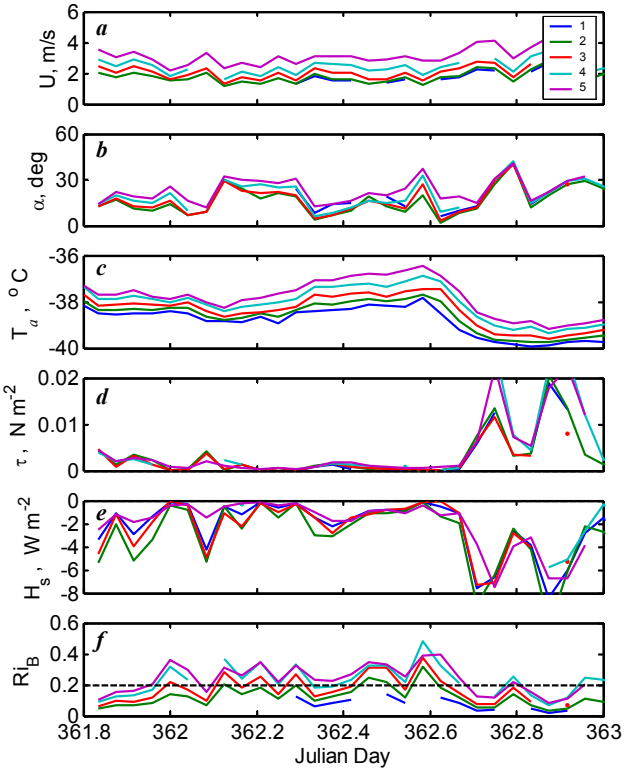

Fig. 1. Time series of the (a) the wind speed, (b) the true wind direction, (c) the air temperature, (d) the downwind stress, (e) the sensible heat flux, and (f) the bulk Richardson number (1) measured at the five levels during the polar night, JD 361-362 (December 27-28, 1997).

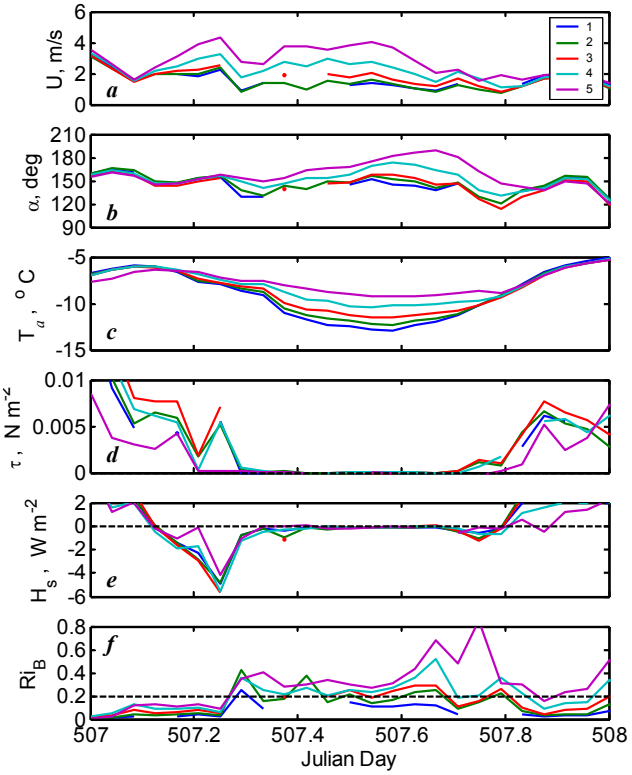

Fig. 2. Same as Figure 1 but for data obtained during the sunlit period, JD 507 (May 22, 1998). Evolving Ekman-type spirals observed during this day for five hours from 12.00 to 16.00 UTC is given in Grachev et al. (2002).

where T_v is the virtual temperature, u is the wind speed at the level z, $\Delta\theta$ and Δq are differences in the potential temperature and the specific humidity between the surface and the reference level z. Based on the SHEBA data, Grachev et al. (2002), show that a value of the bulk Richardson number of about 0.2 may be considered critical, $\mathrm{Ri}_{B\,cr}$. According to Figs. 1 and 2, as the bulk Richardson number (1), approaches its critical value $\mathrm{Ri}_{B\,cr} \approx 0.2$, turbulence decays and vertical fluxes vanish. In this regime, the surface layer is affected by the turning effects of the Coriolis force, which causes veering of the wind vector at the different levels (Figs. 1b and 2b). The observed wind speed shows features of the Ekman spiral even near the surface. The wind vector decays and turns clockwise with decreasing height as expected for the Northern Hemisphere. Figures 1 and 2 shows a layered structure, where the supercritical regime ($\mathrm{Ri}_B \gtrsim 0.2$) is associated with the upper sonic levels, and weak turbulence occupies the near-surface layer (usually 1–3 lowest sonic levels). Therefore the turbulent Ekman layer occupies the lower levels where the turbulence is more or less continuous ($\mathrm{Ri}_B \lesssim 0.2$) and the intermittently stratified Ekman layer usually occupies the levels 4 and 5 with collapsed turbulence (no turbulence). In this regime the surface layer (continuous turbulence) may be very shallow, less than 5 m. Figures 1 and 2 also show some more extreme cases where turbulence collapses at four or even at all five levels. The SHEBA data presented in Fig. 2 provide an example of the evolving SBL passing through the scaling regimes described by Grachev et al. (2002). During the evening transition period (JD ≈ 507.2), the SBL state is changed from the weakly stable regime to the supercritical stable regime (or the intermittently turbulent Ekman layer). Toward the morning hours (JD ≈ 507.8), the SBL passes these regimes in the reverse order.

3. TURBULENCE DECAY

According to the SHEBA data, both the downwind stress, τ, and the sensible heat flux,

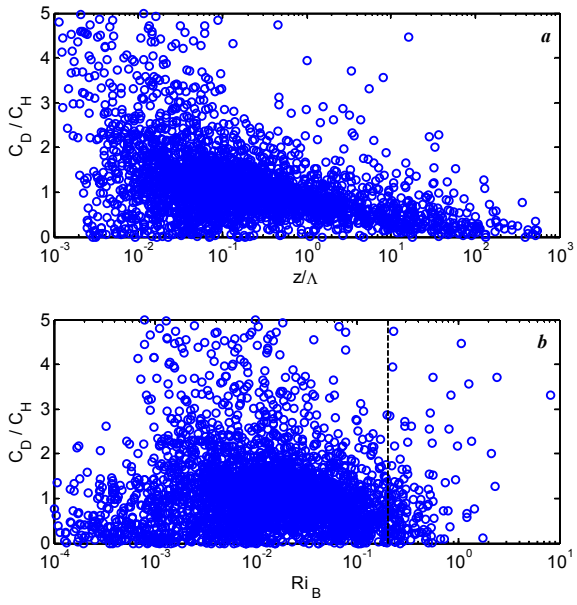

Fig. 3. Ratio C_D / C_H versus (a) a local stability parameter, z/Λ, and (b) the bulk Richardson number. Vertical dash line in the bottom panel corresponds to the critical Richardson number Ri_B = 0.2. Open circles are individual 1-hr averaged data based on the median fluxes and mean meteorological variables for the five levels.

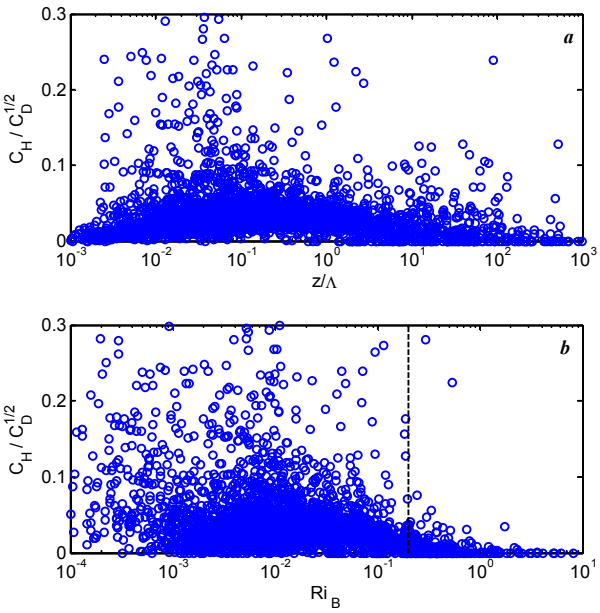

Fig. 4. Same as Figure 3 but for ratio $C_H / C_D^{1/2}$.

H_S, decrease rapidly with increasing stability, but the stress falls faster than the heat flux, i.e. small but still significant heat flux (several Watts per square meter) and negligibly small stress characterize this situation (Grachev et al. 2002). Thus mechanical turbulence decays faster than temperature fluctuations. This effect is also observed in the time series presented in Figs. 1 and 2 (e.g. JD 362.3 and 507.4). In the terms of the drag coefficient, C_D, and the Stanton number, C_H, according to our SHEBA data $C_D / C_H \to 0$ but $C_H / C_D^{1/2} \to 0$ as z/Λ (or Ri_B) $\to \infty$ (Figs. 3 and 4). Thus, in the very stable case the Stanton number falls slower than the drag coefficient but faster than $C_D^{1/2}$. In the stability parameter z/Λ, the local Obukhov length Λ is based on the local fluxes at height z rather than on the surface values.

Figure 5 shows dependence of the $T_* = -\langle T'w' \rangle / u_*$ upon stability. Behavior of T_* is similar to H_S [see Fig. 1 in Grachev et al. (2002)]/ but with the opposite sign since T_* > 0 in the stable conditions. In the near neutral case T_* $\to$ 0 since $\langle T'w' \rangle \approx 0$ and $u_* \neq 0$. With further increasing stability T_* increases and reaches a maximum and $T_* \to 0$ in the very stable case. The last result is not a trivial one since both $\langle T'w' \rangle$ and $u_* \to 0$ as z/Λ (or Ri_B) $\to \infty$.

According to Grachev et al. (2002), the *uw*-covariance falls as a parabolic function since both u' and w' (or standard deviations σ_u and σ_w)

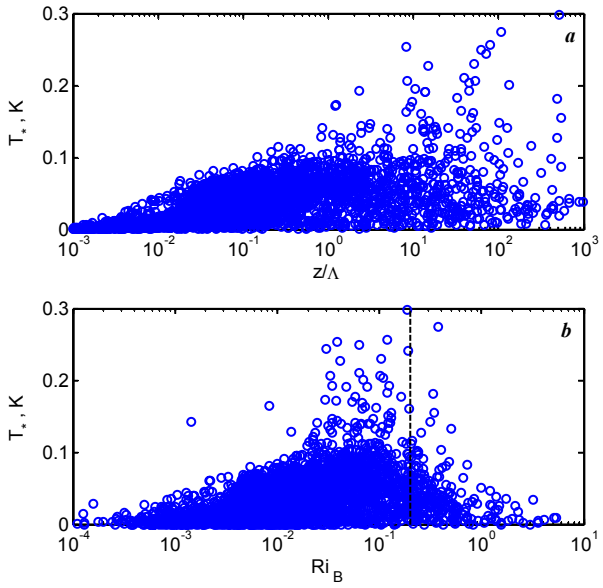

Fig. 5. Same as Figure 3 but for $T_* = -\langle T'w' \rangle / u_*$.

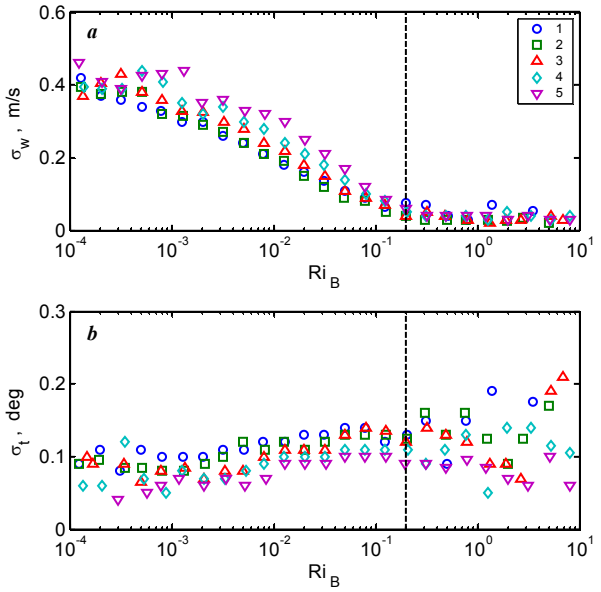

Fig. 6. Plots of the bin-averaged standard deviations of the (a) the vertical wind speed component, and (b) the air temperature for levels 1–5 versus the bulk Richardson number. Vertical dash line in the bottom panel corresponds to the critical Richardson number Ri_B *= 0.2.*

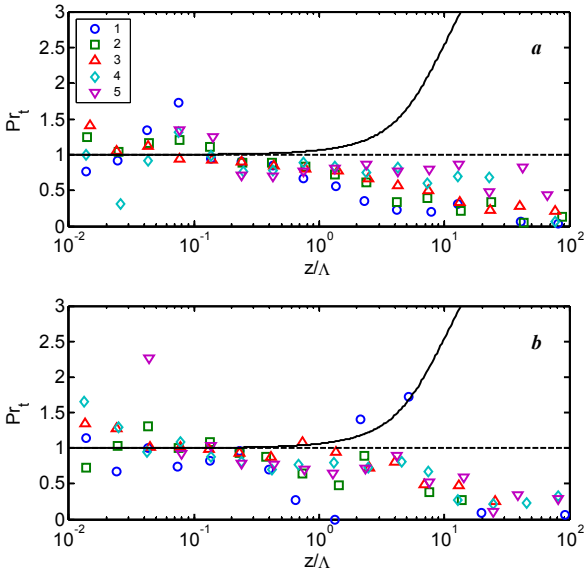

Fig. 7. Plots of the bin-averaged turbulent Prandtl number (2) at five levels versus z/Λ *during (a) the polar 'winter' (265 < JD < 445), and (b) the polar 'summer' (all other JD) computed for air-surface temperature difference* $T_{a\,m} - T_o$ *> 0.5°. Solid line is derived from the Beljaars and Holtslag (1991) formula.*

approach to zero. At the same time the heat flux decreases as a linear function since only $w' \to 0$, while t' (or σ_t) is small but is still a finite value even in the very stable case (Fig. 6). This behavior of σ_t may be associated with a surface that is inhomogeneous in temperature and with the strong temperature vertical gradient.

Turbulence characteristics and vertical profiles of wind velocity and temperature over an inhomogeneous land surface were described by Kukharets and Tsvang (1998). Small-scale spatial variations of the surface temperature (up to several degrees) lead to the higher values for σ_t / T_* than predicted by the Monin–Obukhov theory for a uniform surface. Andreas et al. (1998) reported similar behavior for humidity statistics over a surface with vegetation that was patchy at meter scales. The surface around the main tower is multi-year pack ice with varying thickness and the surface is composed of ice (of different types, thickness, salinity etc.), snow (of different depth, age etc.), meltponds and even leads. These surface patches are characterized by different albedo, thermal capacity and conductivity and therefore may have a different temperature. Overland et al. (2000) have, in fact, documented a 10°C range in surface temperatures in the vicinity of the SHEBA camp during the winter. Paulson and Pegau (2001) reported that the surface temperature of the open water during the summer is about 2° C whereas the ice surface temperature cannot go above 0°C. These 'hot' and 'cold' spots generate small-scale advection which enhances temperature fluctuations and the sensible heat flux. This contribution is small but enough to cause a different decaying of the momentum and the sensible heat flux.

The above mechanism of the asymmetric decay of the momentum and heat fluxes leads to a decrease of the turbulent Prandtl number with increasing stability (Fig. 7). The turbulent Prandtl number, Pr_t, is defined as (e.g. Andreas 2002)

$$\mathrm{Pr}_t = \nu_t / k_t \equiv \varphi_h / \varphi_m \qquad (2)$$

where ν_t is the turbulent viscosity and k_t is the turbulent thermal conductivity (φ_m and φ_h are the non-dimensional universal functions for velocity and potential temperature gradients in the Monin-Obukhov theory). The obtained result Pr_t < 1 indicates that the heat transfer is more efficient than momentum transfer for the very stable regime due to the temperature-inhomogeneous surface.

Unlike Figs. 1–6, the SHEBA data in Fig. 7 are sorted for polar 'winter' and the polar 'summer' conditions. The polar 'winter' lasts from 22

September 1997 until 21 March 1998, or JD265–JD 445 (from autumnal till vernal equinox). Polar 'summer' is all other days. Although the surface during the polar 'winter' is more uniform (no melt ponds), the turbulent Prandtl number is still decreasing with increasing stability (Fig. 7a), although Pr_t decays more slowly than for the polar 'summer' (Fig. 7b). Our results clearly indicate that observed Pr_t behavior is associated with the influence of the temperature-inhomogeneous surface. According to Fig. 7a, the turbulent Prandtl number at higher levels (4 and 5) is closer to unity than at the lower levels. This is due to the fact that the temperature fluctuations (Fig. 6b) and heat transfer associated with the near-surface small-scale advection fall with height, and Pr_t obtained at the higher levels are less affected by this mechanism.

Our result Pr_t < 1 is consistent with Howell and Sun's (1999) data but disagrees with the measurements of Kondo et al. (1978), Yagüe et al. (2001), Beljaars and Holtslag's (1991) formula, and Zilitinkevich and Calanca's (2000) model. One may speculate that Pr_t, φ_m, and φ_h do not have universal behavior in very stable conditions. The turbulent Prandtl number describes the difference in turbulent transfer between momentum and sensible heat. Similarity in the turbulent mixing of momentum and heat suggests Pr_t = 1. However, physical processes overlooked in the Monin-Obukhov theory (e.g. internal gravity waves, Kelvin-Helmholtz billows, upside-down SBL, radiative flux divergence, temperature-inhomogeneous surface) may increase only momentum transfer (Pr_t > 1), only heat transfer (Pr_t < 1), or may produce a mixed effect and therefore violate similarity. Internal gravity waves in the SBL are presumed to lead to Pr_t > 1 (e.g. Zilitinkevich and Calanca, 2000). A surface with inhomogeneous temperature should increase the heat transfer and cause Pr_t < 1.

4. CRITICAL RICHARDSON NUMBER

Another uncertainty exists with regard to the determination of the critical Richardson number. According to the commonly accepted theoretical expectations, surface-layer turbulence, and therefore fluxes, collapses when the Richardson number is greater than its critical value. Several different definitions of the Richardson number are widely used. The flux Richardson number, Rf, and the gradient Richardson number, Ri, are defined by

$$\mathrm{Rf} = \frac{g}{T_v}\frac{<w'T_v'>}{<u'w'>(dU/dz)} \equiv \frac{z/L}{\varphi_m} \qquad (3)$$

$$\mathrm{Ri} = \frac{g}{T_v}\frac{d\theta_v/dz}{(dU/dz)^2} \qquad (4)$$

The vertical wind and temperature gradients in (3) and (4) were obtained by fitting a second-order polynomial regression in $\ln z$ and taking the derivative with respect to z at the level of interest. Close to the surface, it is convenient to use a bulk Richardson number (1). Accordingly, various versions of the Richardson number based on (1), (3) and (4) specify different critical values. The classical estimate of the critical Richardson number Ri_{cr} = 0.25 is based on (4) and is derived from the perturbation analysis. Andreas (2002) and Zilitinkevich and Baklanov (2002) recently reviewed different versions of the critical Richardson number. These surveys show that the critical Richardson number obtained in different studies varies in the wide range, e.g. Ri_{cr} = 0.15 – 0.55 (Zilitinkevich and Baklanov 2002).

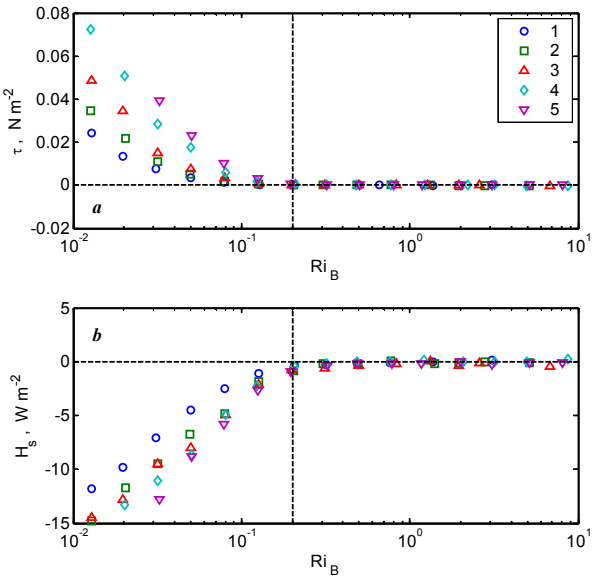

Fig. 8. Plots of the bin-averaged (a) momentum flux and (b) sensible heat flux at five levels versus the bulk Richardson number (1) during the polar 'winter' (265 < JD < 445). Vertical dash lines correspond to the critical Richardson number Ri_B *= 0.2.*

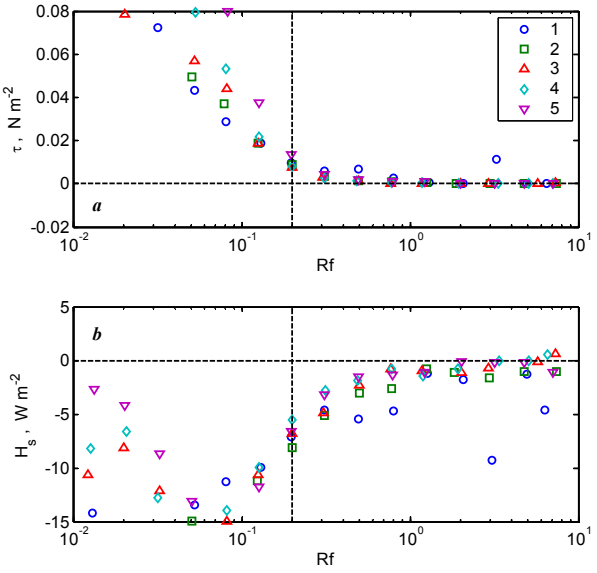

Fig. 9. Same as Figure 8 but for the flux Richardson number (3).

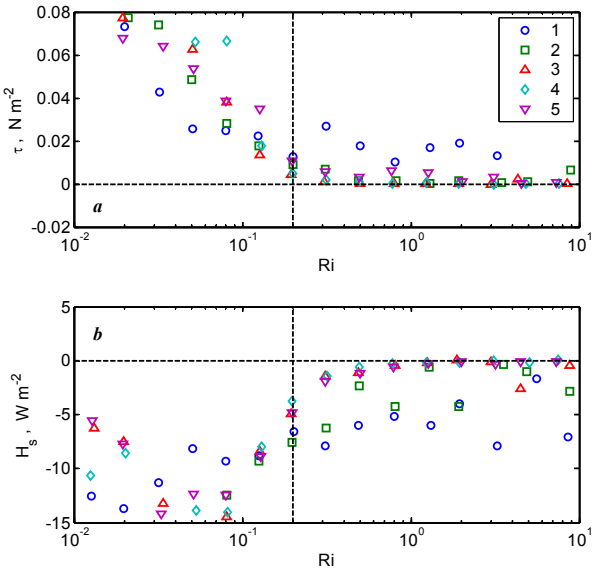

Fig. 10. Same as Figure 8 but for the gradient Richardson number (4).

We consider the critical Richardson number based on the decay of the downwind stress, τ, and the sensible heat flux, H_S. Using the fluxes is preferable to velocity and temperature variances for studying decaying turbulence since noise is not correlated in the covariances $<u'w'>$ and $<T'w'>$. In order to reduce the influence of the inhomogeneity in the surface temperature, we consider only the 'polar' winter period, i.e. JD265–JD 445. Figure 8 shows decaying momentum and heat fluxes as function of the bulk Richardson number (1). According to Fig. 8, a bulk Richardson number of about 0.2 may be considered as the critical value; that is $\mathrm{Ri}_{B\,cr} \approx 0.2$. However, τ is collapsed at a value of Ri_B slightly less than 0.2, and H_S at a value slightly greater than 0.2 (see discussion in the Section 3).

Figures 9 and 10 show similar plots for Rf (3) and Ri (4). For both Rf and Ri, significant turbulent fluxes were still observed when the Richardson number exceeded the "critical" value 0.2. The momentum flux disappears at about $\mathrm{Rf} \approx \mathrm{Ri} \approx$ 0.3–0.5, whereas the sensible heat flux almost ceases at higher values, $\mathrm{Rf} \approx \mathrm{Ri} \approx$ 0.8–1.0 (Figs 9 and 10). Furthermore, determining Rf_{cr} is complicated due to self-correlation (e.g., Mahrt, 1999) since the fluxes appear in both the axes variables (Fig. 9). However, there is no artificial correlation in the coordinates when the fluxes are plotted versus Ri_B and Ri (Figs. 8 and 10). The flux and gradient Richardson numbers, especially for levels 1 and 2 (Figs. 9 and 10), show more scatter than the bulk Richardson number (Fig. 8) because of the influence of advective flows associated with the inhomogeneity in the surface temperature on the gradient and flux calculations in (3) and (4). Thus for practical purposes, based on the SHEBA data, we recommend using the bulk Richardson number (1) and its critical value $\mathrm{Ri}_{B\,cr} \approx 0.2$ (Fig. 8) rather than the flux and the gradient Richardson numbers, (3) and (4).

5. CONCLUSIONS

We discussed the turbulence behavior near the critical Richardson number based on the measurements made during SHEBA. The SBL that we observed most often may be characterized as the traditional boundary layer or surface-flux dominated SBL, where turbulence is generated by surface roughness (cf. Mahrt and Vickers, 2002). The atmospheric boundary layer over the Arctic is often stable stratified and the very stable regimes are usually associated with the light winds, less than about 2 m/s (Figs. 1 and 2). As the Richardson number approaches its critical value, turbulence decays and vertical fluxes vanish. However, the stress falls faster than the heat flux. In other words, small but still significant heat flux (several Watts per square meter) and negligibly small stress characterize this situation, which may be important for the Arctic heat budget.

This asymmetric decay of the turbulent fluxes may be associated with a surface that is inhomogeneous in temperature. The floe around our main SHEBA tower was multi-year pack ice with surface features that changed with season. It went from compact and totally snow covered in winter to bare ice with melt ponds and leads with large area fraction in the height of summer. These latter surface patches have different albedo, thermal capacity, and conductivity and therefore have a different surface temperature than the bare ice. These 'hot' and 'cold' spots generate small-scale advection which enhances temperature fluctuations and the sensible heat flux. As a result, the temperature standard deviation, σ_t, in the very stable case is small but is still a finite value, while σ_w approaches to zero (Fig. 6).

According to our SHEBA data, a bulk Richardson number (1) of about 0.2 may be considered as the critical value; that is $\mathrm{Ri}_{B\,cr} \approx 0.2$ (Fig. 8). However, significant turbulent fluxes were still observed when the flux and the gradient Richardson numbers, (3) and (4), exceeded the "critical" value 0.2, Figs. (9) and (10).

6. ACKNOWLEDGEMENTS

The U.S. National Science Foundation supported this work with awards to the NOAA Environmental Technology Laboratory (OPP-97-01766), the Cooperative Institute for Research in Environmental Sciences, University of Colorado (OPP-00-84322, OPP-00-84323), the U.S. Army Cold Regions Research and Engineering Laboratory (OPP-97-02025, OPP-00-84190), and the Naval Postgraduate School (OPP-97-01390, OPP-00-84279). The U.S. Department of the Army provided additional support to Andreas and Jordan through projects at CRREL.

7. REFERENCES

Andrdeas, E. L, 2002: Parameterizing scalar transfer over snow and ice: A review. *J. Hydrometeor.*, **3**(4), 417–432.

Andrdeas, E. L, R. J. Hill, J. R. Gosz, D. I. Moore, W. D. Otto, and A. D. Sarma, 1998: Statistics of surface-layer turbulence over terrain with metre-scale Heterogeneity. *Boundary-Layer Meteorol.*, **86**, 37–408.

Andreas, E. L., C. W. Fairall, P. S. Guest, and P. O. G. Persson, 1999: An overview of the SHEBA atmospheric surface flux program. *13th Symposium on Boundary Layers and Turbulence*. Dallas, TX, Amer. Meteorol. Soc., 550–555.

Beljaars, A. C. M. and A. A. M. Holtslag, 1991: Flux parameterization over land surfaces for atmospheric models. *J. Appl. Meteorol.* **30**, 327 – 341.

Grachev, A. A., C. W. Fairall, P. O. G. Persson, E. L Andreas, and P. S. Guest, 2002: Stable boundary - layer regimes observed during the SHEBA experiment. *15th Symposium on Boundary Layers and Turbulence*. Wageningen, The Netherlands, Amer. Meteorol. Soc., Proceedings, 374 – 377.

Howell, J. F. and J. Sun, 1999: Surface-layer fluxes in stable conditions. *Boundary-Layer Meteorol.*, **90**(3), 495–520.

Kondo, J., O. Kanechika, and N. Yasuda, 1978: Heat and momentum transfers under strong stability in the Atmospheric Surface Layer. *J. Atmos. Sci.* **35**(6), 1012 – 1021.

Kukharets, V. P. and L. R. Tsvang, 1998: Atmospheric turbulence characteristics over a temperature-inhomogeneous land surface. Part I: Statistical characteristics of small-scale spatial inhomogeneities of land surface temperature', *Boundary-Layer Meteorol.* **86**, 89–101.

Mahrt, L., 1999: Stratified atmospheric boundary layers. *Boundary-Layer Meteorol.*, **90**(3), 375–396.

Mahrt, L. and D. Vickers, 2002: Contrasting vertical structures of nocturnal boundary layers. *Boundary-Layer Meteorol.* **105**, 351–363.

Overland, J. E., S. L. McNutt, J. Groves, S. Salo, E. L Andreas, and P. O. G. Persson, 2000: Regional sensible and radiative heat flux estimates for the winter Arctic during the Surface Heat Budget of the Arctic Ocean (SHEBA) experiment. *J. Geophys. Res.,* **105**, 14,093–14,102.

Paulson, C. A., and W. S. Pegau, 2001: The summertime thermohaline evolution of an Arctic lead: Heat budget of the surface layer. *Sixth Conf. on Polar Meteorology and Oceanography*, San Diego, CA, Amer. Meteorol. Soc., Proceedings, 271 – 274 .

Persson, P. O. G., C. W. Fairall, E. L. Andreas, P. S. Guest, and D. K. Perovich, 2002: Measurements near the Atmospheric Surface Flux Group tower at SHEBA: Near-surface conditions and surface energy budget. *J. Geophys. Res.* **107**(C10), 8045, doi: 10.1029/2000JC000705.

Yagüe, C, G. Maqueda, and J. M. Rees, 2001: Characteristics of turbulence in the lower atmosphere at Halley IV station, Antarctica. *Dyn. Atmos. Ocean*, **34**, 205–223.

Zilitinkevich, S. S., and A. Baklanov, 2002: Calculations of the height of the stable boundary layer in practical applications. *Boundary-Layer Meteorol.*, **105**, 389–409.

Zilitinkevich, S. S., and P. Calanca, 2000: An extended similarity-theory for the stably stratified atmospheric surface layer. *Quart. J. Roy. Meteorol. Soc.*, **126**, 1913–1923.